JOURNAL OF VIROLOGY, Nov. 1978, p. 590-599
0022-538X/78/0028-0590$02.00/0

Vol. 28, No. 2
Printed in U.S.A.

Selective Degradation of Newly Synthesized Nonmessenger Simian Virus 40 Transcripts

NANCY H. CHIU,* MICHAEL F. RADONOVICH, MARILYN M. THOREN, AND NORMAN P. SALZMAN

Laboratory of Biology of Viruses, National Institute of Allergy and Infectious Diseases, National Institutes of Health, Bethesda, Maryland 20014

Received for publication 28 March 1978

By pretreating simian virus 40-infected BSC-1 cells with glucosamine, [^{3}H]uridine labeling of both cellular and viral RNA can be halted instantaneously by addition of cold uridine. We have studied the fate of pulse-labeled viral RNA from cells at 45 h postinfection under these conditions. During a 5-min period of labeling, both the messenger and nonmessenger regions of the late strand were transcribed. After various chase periods, nuclear viral species which sediment at 19, 17.5, and 16S were observed. Nuclear viral RNA decays in a multiphasic manner. Of the material present at the beginning of the chase period, 50% was degraded rapidly with a half-life of 8 min (initial processing). This rapidly degraded material was that fraction of the late strand which did not give rise to stable late mRNA species. Forty percent was transported to the cytoplasm, and 10% remained in the nucleus as material which sedimented in the 2 to 4S region. These 2 to 4S viral RNAs had a half-life of 3 h, and hybridization studies suggest that they are in part coded for by the late-strand nonmessenger region and are derived from the initial nuclear processing step. Another part is coded for by the late-strand messenger region and may be generated by some subsequent nuclear cleavages of 19S RNA into 17.5 and 16S RNAs. Transport of nuclear viral RNA into the cytoplasm was detected after a 5-min pulse and a 7-min chase. The maximum amount of labeled viral RNA was accumulated in the cytoplasm after a 30-min to 1-h chase. At least two viral cytoplasmic species were observed. Kinetic data suggest that 19S RNA is transported directly from the nucleus. Whether cytoplasmic 16S is formed by cleavage of 19S RNA in the cytoplasm is not clear. The half-lives of cytoplasmic 19 and 16S RNAs can be approximated as 2 and 5 h, respectively.

Interest in the synthesis and processing of nuclear RNA and their roles in the regulation of cytoplasmic mRNA transcripts (see reviews 9, 16, 17, 21) has prompted us to reexamine the metabolism of the late simian virus 40 (SV40) viral RNAs.

Weinberg et al. (29) have followed the fate of labeled viral RNAs by using actinomycin D to inhibit further RNA synthesis. They showed two major classes of late SV40-specific mRNA's in the cytoplasm that sedimented with values of 16 and 19S. Aloni et al. (3) have examined late mRNA's after various periods of pulse-labeling and studied the fate of 3-h labeled cytoplasmic viral RNAs after enucleation of infected cells. They report two predominant species of viral RNA, 16 and 19S, with half-lives of 6 and 3 h, respectively.

We have treated SV40-infected cells with glucosamine before labeling and added cold uridine and glucosamine after a brief pulse-labeling period (24, 30). By using this technique, good pulse-chase conditions were established. This method is preferred to the use of actinomycin D, which may inhibit RNA chain elongation as well as processing (15). Under pulse-chase conditions with glucosamine, we have examined the processing, transport, and degradation of a relatively homogeneous population of nuclear viral RNA molecules labeled during a brief pulse. The sizes and sequence specificities of viral RNAs in both nucleus and cytoplasm at different time intervals of chase have been determined.

MATERIALS AND METHODS

Cells and virus. A plaque-purified stock of wild-type SV40 (strain 776) was grown in a BSC-1 line of African green monkey kidney cells with an input multiplicity of 0.01 PFU/cell. For all experiments, BSC-1 cells were grown at 37°C in 150-mm plastic petri dishes with Eagle medium supplemented with 2 mM glutamine, streptomycin (1.35 mg/ml), penicillin (0.62 mg/

ml), chlortetracycline (0.2 mg/ml), mycostatin (500 U/ml), and 10% fetal calf serum. Confluent monolayers of cells were infected with virus at an input multiplicity of 20 PFU/cell. The infected cells were then grown at 37°C in the same medium except that it contained 2% fetal calf serum.

Pulse and chase experiments. At 45 h postinfection, cells were preincubated for 80 min at 37°C with 20 mM glucosamine in Eagle medium containing 2% fetal calf serum. The cultures were then rinsed with prewarmed complete Hanks balanced salt solution and labeled for 5 min at 37°C with 100 μCi of [^{3}H]uridine per ml (Schwarz/Mann; 33 Ci/mmol) in complete Hanks solution. In the chase experiments, the cultures were rinsed with prewarmed complete Hanks solution and incubated with prewarmed fresh Eagle medium containing 2% fetal calf serum, 20 mM glucosamine, and 1 mM cold uridine at 37°C for varying time intervals.

Cell fractionation and RNA extraction. Cytoplasmic and nuclear fractions were prepared by hypotonic reticulocyte standard buffer solution swelling and Dounce homogenization (20). After disrupting the cells, the cytoplasm was obtained by low-speed centrifugation at 4°C. Final concentrations of 100 μg of RNase inhibitor polyvinyl sulfate per ml and 0.5% sodium dodecyl sulfate were added to the supernatant. The cytoplasmic RNA was then extracted from the supernatant fluid with chloroform:phenol:isoamyl alcohol (50:50:1).

The nuclei were washed further with phosphate-buffered saline containing 1% Nonidet P-40 and 0.5% sodium deoxycholate. Heterogeneous nuclear RNA was extracted from the nuclear pellet by the procedures of Scherrer (23) and Meissner et al. (19). A nuclear pellet from one petri dish was resuspended in 0.5 ml of 2 mM $MnCl_2$–5 mM Tris-hydrochloride (pH 7.0) and held at 0°C for 3 min with 50 μg of RNase-free DNase (31). The solution was adjusted to 10 mM EDTA and mixed with 10 ml of 0.05 M Tris-hydrochloride (pH 7.5) containing 1 mg of polyvinyl sulfate, 0.5 mg of protease K, and 0.4% sodium dodecyl sulfate. After standing at room temperature for 5 min, 10 ml of redistilled phenol was added. The mixture was shaken vigorously in a 60°C water bath for 3 min, 10 ml of chloroform was added, and the mixture was shaken for another 3 min. After centrifugation the aqueous phase was extracted twice more with phenol:chloroform:isoamyl alcohol (vol/vol/vol, 50:50:1). RNA was obtained from the aqueous phase by ethanol precipitation, and the precipitate was redissolved, treated with DNase, and reextracted with phenol–chloroform–isoamyl alcohol. The RNA that was obtained by ethanol precipitation was redissolved in proper buffers for sucrose gradient sedimentation or hybridization.

Sucrose gradient sedimentation. To avoid nuclear RNA aggregation, RNA samples were denatured at room temperature for 30 min in 80% dimethyl sulfoxide, 10% dimethyl formamide, and 10% TES buffer (0.01 M EDTA–0.01 M Tris-hydrochloride [pH 7.4]–0.2% sodium dodecyl sulfate [pH 7.4] [10]). After appropriate dilution, the samples were layered on 5 to 20% sucrose (Schwarz/Mann; RNase free) gradients containing 0.05 M NaCl in TES buffer. The gradients were centrifuged in an SW 41 rotor at 39,000 rpm for 5.5 h at 20°C. Tubes were punctured at the bottom, and 0.3-ml fractions were collected.

Hybridization. For hybridization of [^{3}H]RNA with total SV40 DNA, viral DNA was isolated from purified virions, and 30 μg was immobilized on the 30-mm nitrocellulose filters (Schleicher and Schuell) as described by May et al. (18). For hybridization across the sucrose gradient, minifilters were used. Square minifilters (3 by 3 mm) were cut from the 30-mm SV40 DNA (30 μg/filter) immobilized filters. Blank minifilters containing no DNA were cut in the same way from 30-mm blank filters. Hybridizations were performed in 4× SSC (1× SSC = 0.15 M NaCl–0.015 M Na_3 citrate) at 60°C for 18 h, and then the filters were washed, RNase treated, and washed again. The filters were dried and counted in toluene-based scintillant.

To determine the relative amounts of RNA synthesized from messenger and nonmessenger regions of the early and late strands of SV40 DNA, [^{3}H]RNA samples were hybridized to separated strands of SV40 DNA fragments immobilized on nitrocellulose strips. The technique is described in detail by Birkenmeir et al. (6). In this procedure, SV40 DNA was cleaved by restriction enzymes *Bam* I and *Hpa* II into two fragments: fragment A (map unit, 0.16 to 0.735; clockwise) and fragment B (0.735 to 0.16 map units; clockwise). More than 95% of the early viral mRNA sequences are mapped within the A fragment (5). The two major late viral mRNA's 16 and 19S extend from 0.94 to 0.17 and 0.775 to 0.17 map units, respectively. The leader sequences of the 16S RNA extend from 0.72 to 0.76 map units (11). Therefore, more than 90% of the late viral mRNA sequences are mapped within the B fragment. By denaturation and gel electrophoresis of this DNA digest, the four single-stranded fragments can be separated. These fragments, in increasing order of mobility, are EA (A fragment, early-strand messenger region), LA (A fragment, late-strand, anti-early messenger region), LB (B fragment, late-strand messenger region), and EB (B fragment, early-strand, anti-late messenger region). The four fragments are transferred from the agarose gels to nitrocellulose sheets as described by Southern (27). Usually, a sheet 10 cm wide by 7 cm long contained 10 μg of SV40 DNA and was divided into six strips. To mimimize possible secondary structures, labeled RNA samples in 0.01× SSC were heated at 90°C for 10 min before use. Hybridizations were performed at 68°C in 6× SSC for 18 h. The strips were washed, RNase treated, and washed again with 1× SSC. Dried strips were momentarily immersed in toluene containing 2,5-diphenyloxazole (20%, wt/vol) and subjected to autoradiography with Kodak Royal X-Omat film. The densitometric tracings were obtained by scanning the autoradiograms in a Gilford spectrophotometer at 560 nm. The areas under the peaks were used to calculate the percentages of RNA hybridizing to these single-stranded DNA fragments.

RESULTS

Kinetics of labeling and processing (decay and export) of nuclear viral RNA. The incorporation of isotope into the nuclear RNA or into virus-specific nuclear RNA after 1.5-, 3-,

and 5-min pulses was 0.82×10^6, 1.65×10^6, and 5.08×10^6 and 2.35×10^4, 4.71×10^4, and 13.36×10^4 cpm/dish, respectively. Once the chase started, no further uptake of isotope was observed (Fig. 1). By monitoring the uptake of radioactivity into transfer RNA of cultured *Drosophila* cell lines, an abrupt cessation of labeling under the same pulse-chase condition has also been demonstrated by Levis and Penman (15).

The semilog plot of the decay curve of the total nuclear RNA is multiphasic (Fig. 1). About half the labeled nuclear cellular RNA was degraded after a 1-h chase, and 50% of the material that remained after a 1-h chase was degraded during the following 5 h of chase. The relative amounts of labeled nuclear viral RNA that remained after a 5-min pulse period and chase periods of 0, 5, 10, 15, 30, 60, 180, and 360 min were 1, 0.65, 0.43, 0.31, 0.28, 0.17, 0.12, and 0.08, respectively (Table 1). The semilog plot of the decay curve of viral nuclear RNA also appears to be multiphasic (Fig. 1). Fifty percent of viral nuclear RNA had a half-life of 8 min, which is much shorter than any significant fraction of the cellular nuclear RNA. The remaining viral RNA decayed more slowly, and it can be further divided into at least two categories. Eighty percent of the slowly decaying RNA had a half-life of 40 min, and 20% had a half-life of 3 h.

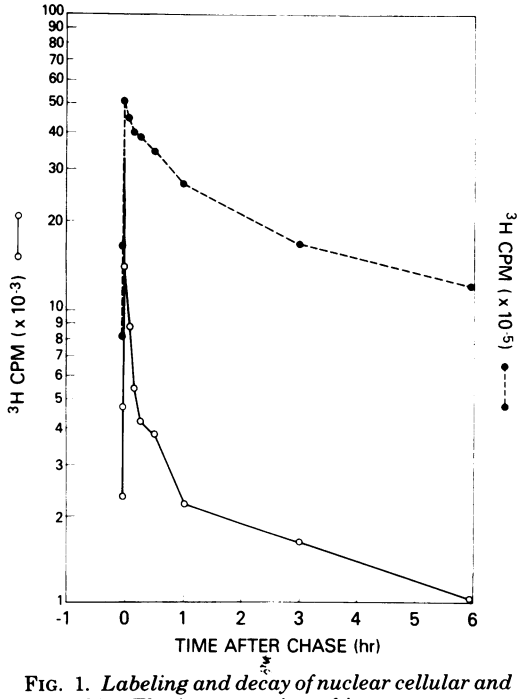

FIG. 1. *Labeling and decay of nuclear cellular and viral RNAs. The incorporation of isotope was measured after 1.5-, 3-, and 5-min pulses. The 5-min pulse corresponds to the zero-time chase. Incorporation was also measured after 5-, 10-, 15-, 30-, 60-, 180-, and 360-min chases. Chase values are from Table 1. Total nuclear RNA (●- - -●); nuclear viral RNA (○——○).*

The sizes and sequence specificities of these viral nuclear RNA populations with different half-lives were different. Those results will be presented in the later sections.

Kinetics of labeling and decay of cytoplasmic viral RNA. After a 5-min pulse and a 5-min chase, there was a negligible amount of labeled virus-specific RNA in the cytoplasm. However, the amount of labeled viral RNA detected in the cytoplasm increased rapidly after a 10- to 15-min chase period and reached a maximum after a 30- to 60-min chase (Fig. 2 and Table 1).

A comparison of the initial amount of labeled viral RNA in the nucleus (at 0 min of chase) and the maximal amount of the labeled viral RNA in the cytoplasm (at 60 min of chase) shows that at least 35 to 40% of the initially labeled nuclear viral RNA is transported into the cytoplasm.

After a 1-h chase, only 15% of prelabeled viral RNA remained in the nucleus (Table 1). More than half of this nuclear RNA sedimented at 2 to 4S and cannot be chased into the cytoplasm (see Fig. 3f and below). Therefore, the amount of labeled RNA that enters the cytoplasmic pool after a 1-h chase is small. The labeling and decay curve of cytoplasmic viral RNA (Fig. 2) after a 1-h chase can thus be considered as an approximate decay curve of the prelabeled cytoplasmic viral RNA. The cytoplasmic viral RNA also decays in a complex manner. There was a faster decay of virus-specific counts at a 1- to 3-h chase, and the remaining RNA then decayed more slowly. After an 11-h chase, more than 90% of the transported cytoplasmic viral RNA had been degraded (Fig. 2).

Size distributions of nuclear viral RNAs during the chase. After a 5-min pulse, less than 10% of the synthesized nuclear viral RNA had been degraded. As shown in Fig. 3a, the sizes of these RNAs are heterogeneous, sedimenting between 5 and 26S. After a 5-min chase, 35% of the labeled nuclear viral RNA was degraded. During this time, most of the viral RNAs had sizes between 19 and 26S, with a distinct peak at 19S (Fig. 3b). It seems that processing occurs very rapidly (if not concurrently) as the RNA chains are synthesized. After 10 to 15 min of chase (Fig. 3c and d), viral RNAs with sizes larger than 19S were further reduced in amount. Although 19S RNA was the predominant species, a small reproducible shoulder that sediments at 17.5S was generated. After 30 min of chase (Fig. 3e), the sizes of nuclear viral RNA

TABLE 1. *Kinetics of processing of pulse-labeled SV40 RNAs*[a]

Time after chase	Total triti-ated cellular nuclear RNA cpm ($\times 10^{-6}$)	Total nu-clear SV40 hybridizable cpm ($\times 10^{-4}$)	% of nuclear SV40-spe-cific cpm	Total triti-ated cellular cytoplasmic RNA cpm ($\times 10^{-5}$)	Total cyto-plasmic SV40 hy-bridizable cpm ($\times 10^{-4}$)	% of cyto-plasmic SV40 spe-cific cpm	SV40-specific cytoplasmic RNA cpm/ SV40-specific nuclear RNA cpm
0	5.08	13.36	2.63	6.21	0	0	0
5 min	4.48	8.80	1.96	6.37	0.11	0.17	0.01
10 min	4.00	5.44	1.36	6.57	0.64	0.98	0.12
15 min	3.88	4.20	1.08	6.76	2.57	3.80	0.61
30 min	3.48	3.80	1.09	7.01	3.91	5.58	1.03
60 min	2.68	2.22	0.82	7.55	4.72	6.25	2.15
3 h	1.68	1.61	0.96	9.58	3.28	3.42	2.04
6 h	1.20	1.02	0.85	13.50	2.56	1.90	2.51
11 h				12.72	0.46	0.36	

[a] Confluent monolayers of BSC-1 cells in petri dishes were infected with SV40 virus as described in the text. At 45 h postinfection, cells were treated with glucosamine, pulse-labeled with [^{3}H]uridine, and chased. Nuclear and cytoplasmic RNAs were obtained from one petri dish at each chase time interval. Total counts of nuclear or cytoplasmic RNA was determined by its trichloroacetic acid-precipitable counts. Various portions of total nuclear or cytoplasmic RNA were hybridized to SV40 DNA on filters (5 μg/filter) to obtain a hybridization saturation curve. The percentage of virus-specific RNA contained in the total RNA was determined within the linear range of the plot of hybridizable counts versus total input counts.

became more heterogeneous. A species of 16S RNA was also observed. Meanwhile, small nuclear viral RNAs appeared as a discrete peak sedimenting around 2 to 4S. After a 1-h chase (Fig. 3f), 83% of nuclear viral RNA had been processed, and 2 to 4S RNA gradually replaced large RNA molecules as the predominant nuclear viral species. These small RNAs represent 10% of the initial labeled nuclear viral RNA and decayed with a long half-life of 3 h (Fig. 3g and h).

We have pooled sucrose gradient fractions containing pulse-labeled nuclear RNAs with sizes smaller than 6S after a 1-h chase. They were then hybridized with SV40 DNA filters. The virus-specific RNAs were eluted from the filters and characterized by 7 M urea–12% acrylamide gel electrophoresis (22). The autoradiograms of these gels show that most of the virus-specific small nuclear RNAs are of sizes around 35 nucleotides. There were also some minor species with sizes between 40 and 70 nucleotides.

Size distribution of cytoplasmic viral RNAs during the chase. After a 10- to 15-min chase (Fig. 4a and b), the predominant cytoplasmic species sedimented at 19S. A small amount of 16S RNA is also observed. 19S and 16S became equally abundant after a 1-h chase (Fig. 4d). Although two RNA species were present after a 3- and 6-h chase (Fig. 4e and f), 19S largely diminished, with 16S becoming the predominant species. After an 11-h chase, all of these species were still detectable but in much reduced amounts (Fig. 4g). Very little new labeled 16 to 19S entered the cytoplasmic pool after 1 h of chase. By comparing the counts of

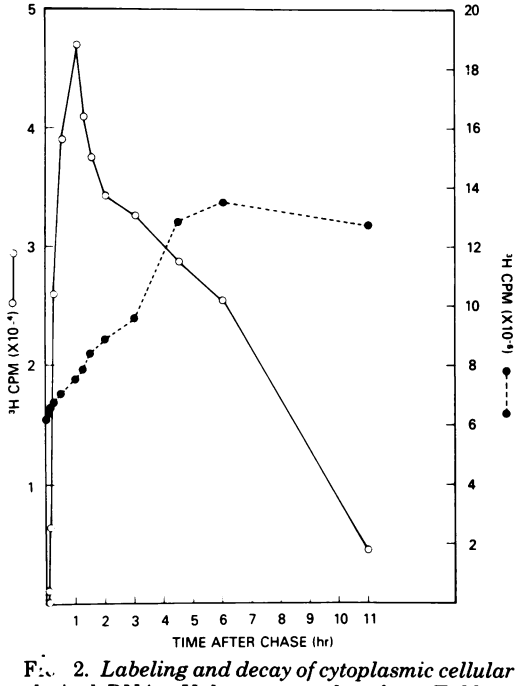

FIG. 2. *Labeling and decay of cytoplasmic cellular and viral RNAs. Values were taken from Table 1. Total cytoplasmic RNA* (●- - -●); *cytoplasmic viral RNA* (○——○).

individual viral species at different time intervals between 1 to 11 h of chase, the half-lives of the cytoplasmic viral 19S and 16S RNAs can be roughly approximated as 2 and 5 h, respectively.

Sequence specificities of nuclear viral RNAs. (i) Primary sequences. Nuclear RNA was isolated after a 6-min pulse. Based on the

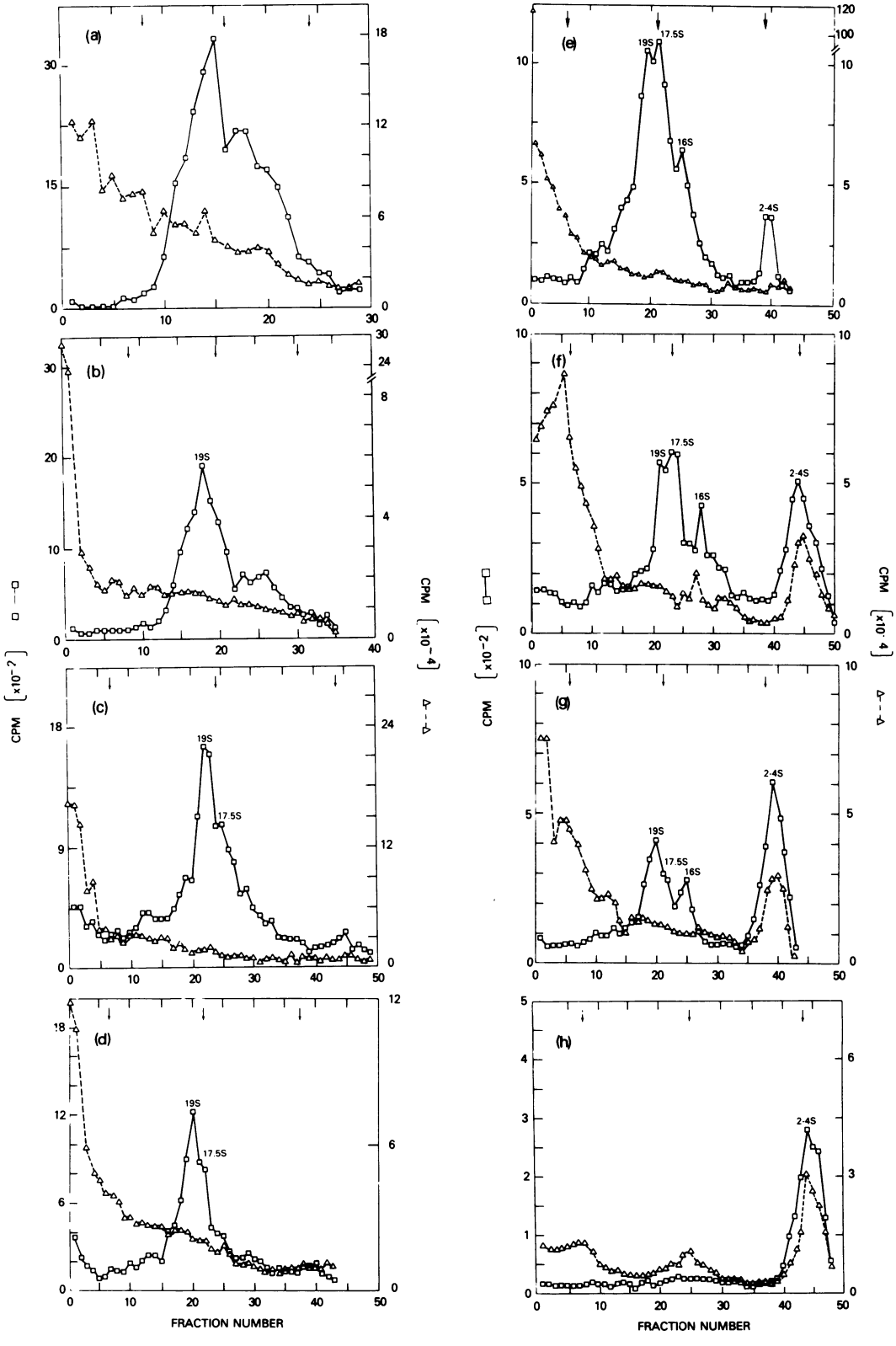
(a)
(b)
(c)
(d)
(e)
(f)
(g)
(h)
19S
17.5S
16S
2-4S
CPM [×10⁻²] □—□
CPM [×10⁻⁴] △--△
FRACTION NUMBER

decay kinetics of nuclear viral RNA, less than 10% of the labeled nuclear viral RNA was processed. To determine the sequence specificity of these primary products, the RNA was hybridized with four single-stranded SV40 DNA fragments as described above.

As shown in Fig. 5b, more than 90% of the nuclear viral RNA is specific to the late strand. The ratio of the late-strand messenger region (LB, map unit 0.735 to 0.16) specific sequences to late-strand nonmessenger region (LA, map unit 0.16 to 0.735) specific sequences is 1.7. There was also a small amount of RNA synthesized from the early strand. Due to the large excess of late RNA, self-annealing of complementary RNA strands may occur in the hybridization solution and mask the detection of such a minor species. By using an alternative hybridization technique such as radioactively labeled early-strand SV40 DNA hybridizing with the cold RNA, trace amounts of early-strand-specific RNA also can be demonstrated. The result is almost identical to the pattern of RNA synthesized in vitro after Sarkosyl extraction of virus-infected nuclei after 45 h postinfection (Fig. 5a). During in vitro RNA synthesis, presumably no processing is involved. Therefore, we conclude that the primary nuclear viral RNA is mainly specific to the late strand, with sequences corresponding to both messenger and nonmessenger regions.

(ii) Nuclear RNAs that remain after the initial 15-min chase period. Pulse-labeled nuclear RNA was isolated after a 15-min chase and hybridized to single-stranded SV40 DNA fragments on nitrocellulose strips. Although the whole late strand was transcribed, the nonmessenger sequences were rapidly degraded within 10 to 15 min of chase (Fig. 5c). The RNA ratio of the messenger sequences (LB) to nonmessenger sequences (LA) is 17. The nuclear viral RNA sequences that were degraded during this chase period cannot be found in the cytoplasm. A small amount of early RNA was now better visualized on the strips due to the disappearance of the late nonmessenger sequences.

(iii) Properties of RNAs sedimenting at 16 to 19S and 2 to 4S that are present in the nucleus. By studying the size distributions of nuclear viral RNAs during various chase periods (Fig. 3), we found that the nuclear viral RNAs of sizes 16 to 19S have a half-life of 40 min, whereas nuclear viral 2 to 4S RNAs have a half-life of 3 h. To determine the sequence specificities of these RNAs, pulse-labeled RNA was isolated after a 1-h chase period. We chose this time point because most nuclear viral RNAs with various discrete sizes are present. The bulk RNA was fractionated through sucrose gradients, and regions of 16 to 19S and smaller than 6S were pooled separately and ethanol precipitated. These RNAs were hybridized to single-stranded SV40 DNA fragments on nitrocellulose strips. As shown in Fig. 6b, more than 80% of the 16 to 19S RNAs were specific to the late messenger region (LB, map unit 0.735 to 0.16).

At 1 h of chase, the small nuclear viral RNAs had a very different sequence specificity than the 16 to 19S species. The relative abundance of sequences specific to early-strand messenger (EA), late-strand nonmessenger (LA), late-strand messenger (LB), and early-strand nonmessenger (EB) regions was 1:1:2:0.5 (Fig. 6a).

DISCUSSION

It is difficult to carry out pulse-chase experiments with RNA because the large intracellular pool of labeled ribonucleotides is not diluted out by the exogenous addition of unlabeled nucleosides or nucleotides. Scholtissek (24) demonstrated that glucosamine can rapidly empty the UTP pool by forming UDP-*N*-acetylglucosamine. Glucosamine has no side effect on the normal metabolism of cellular nonribosomal RNA (15) or viral RNA (30). We have observed normal patterns of cellular ribosomal and nuclear RNA metabolism in sucrose gradients after different chase periods under our conditions.

After having established pulse-chase conditions, we examined the synthesis and metabolic fate of SV40 RNA sequences. In the present study we find that after a 5-min labeling period, more than 90% of the in vivo-synthesized nuclear viral RNA is specific to the late strand at 45 h postinfection. This is in good agreement with the studies obtained from in vitro RNA synthe-

FIG. 3. *Size distributions of nuclear viral RNAs during the chase. At 45 h postinfection, cells were pulse-labeled with [^{3}H]uridine and chased. Nuclear RNA was isolated from one petri dish at each chase time interval. The ethanol precipitates of RNA were resuspended in proper buffer and briefly denatured as described in the text. Small amounts of [^{14}C]uridine-labeled ribosomal RNA were added as markers. Each sample was divided, and half was centrifuged through a 5 to 20% sucrose gradient. Fractions were collected, and 20-μl portions from each fraction were used to determine the total nuclear RNA counts. SV40 DNA (5 μg) on minifilters as well as the blank filters was hybridized with RNA in each fraction to determine the virus-specific counts. The three arrows from left to right are the positions of 28, 18, and 4S RNAs. Sedimentation profiles of pulse-labeled nuclear RNAs at (a) 0 min, (b) 5 min, (c) 10 min, (d) 15 min, (e) 30 min, (f) 1 h, (g) 3 h, and (h) 6 h of chase are presented. Total nuclear RNA (△- - -△); nuclear viral RNA (□——□).*

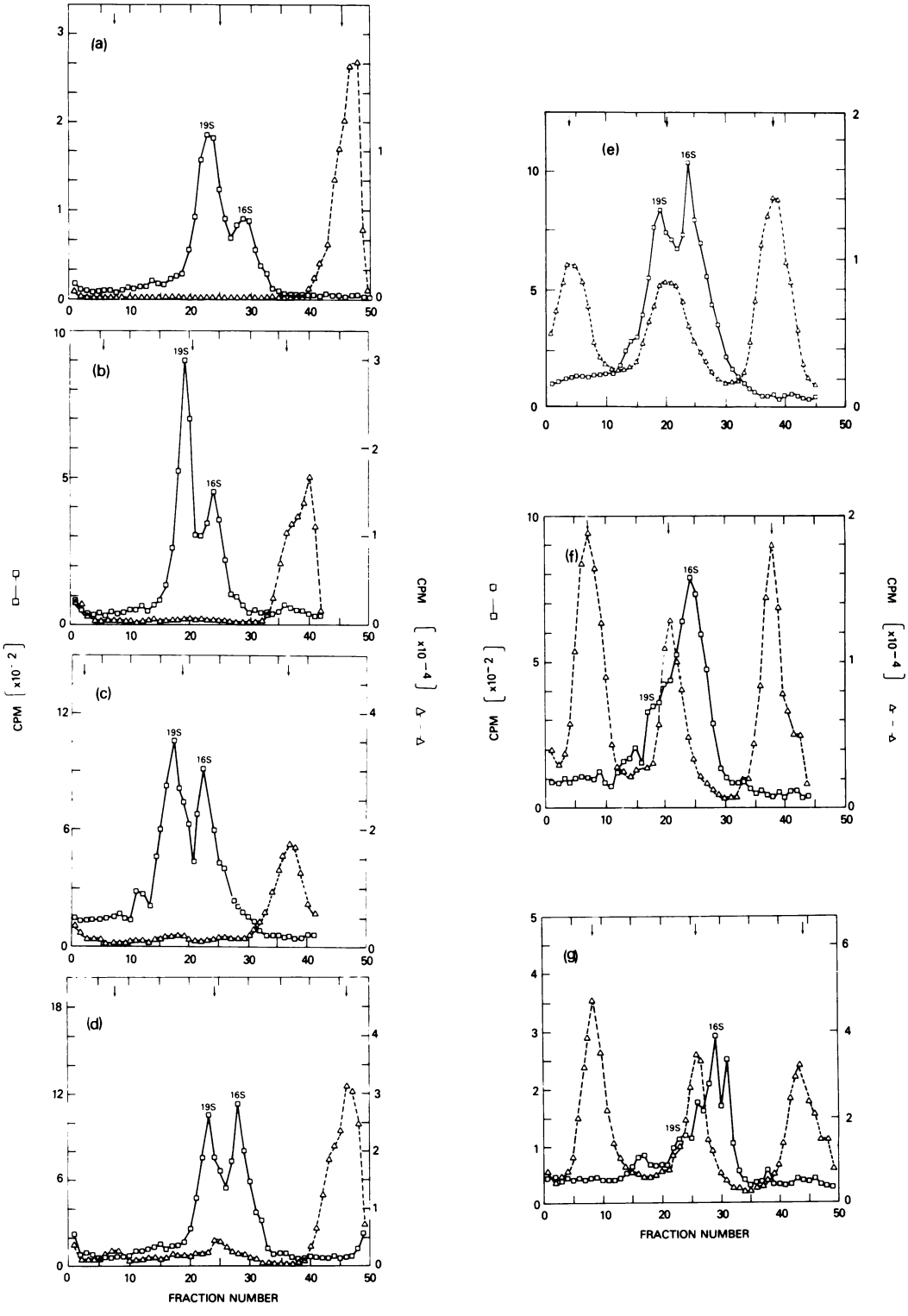

FIG. 4. *Size distributions of cytoplasmic viral RNAs during the chase. Experimental conditions were the same as in Fig. 3 except that cytoplasmic RNAs were examined at (a) 10 min, (b) 15 min, (c) 30 min, (d) 1 h, (e) 3 h, (f) 6 h, and (g) 11 h of chase. Half of the cytoplasmic RNA isolated from one petri dish of infected cells at each chase time interval was centrifuged through sucrose gradient and subsequently hybridized with SV40 DNA minifilters. After the 11-h chase, twice the amount of total RNA was applied to the gradient. Sedimentation profiles of pulse-labeled total cytoplasmic RNAs (△- - -△); cytoplasmic viral RNAs (□——□).*

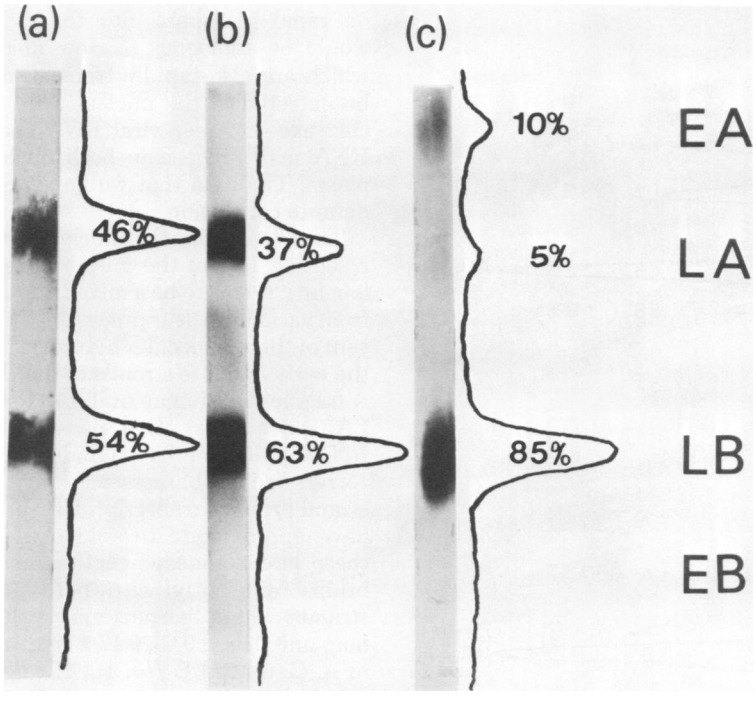

FIG. 5. *Sequence specificities of nuclear viral RNAs with or without processing. Cells were used at 45 h postinfection. Nitrocellulose strips with 1 μg of single-stranded SV40 DNA fragments were used to hybridize with the following RNA samples: (a) in vitro [^{32}P]UTP-labeled RNA synthesized by Sarkosyl extracts of nuclei from two petri dishes of infected cells; (b) in vivo [^{3}H]uridine-, 6-min pulse-labeled nuclear RNA from one petri dish of infected cells; (c) nuclear RNA isolated from one petri dish of infected cells pulsed for 5 min with [^{3}H]uridine and chased for 15 min. The same patterns of hybridization are obtained with lower dilutions of input-labeled RNA samples.*

sis after Sarkosyl extraction of infected nuclei with either SV40 (6, 14, 25) or polyoma virus (8). This in vivo-synthesized primary nuclear viral RNA is complementary to both messenger and nonmessenger regions in equal abundance. Shani et al. (25) and Condit et al. (8) hybridized the in vitro-synthesized RNA with restriction fragments of viral DNA, and they also found that both messenger and nonmessenger regions are transcribed. Processing of SV40 nuclear RNA can be divided into at least two steps. Although the whole viral late strand is transcribed in the nucleus at 45 h postinfection, the nonmessenger region (LA, map unit 0.16 to 0.735) is degraded into an acid-soluble form with a half-life of 8 min. We call this the initial nuclear processing step. There are at least three viral RNA species which appear in the nucleus after a 5-min pulse and a 10- to 30-min chase. The 19S is first observed, and then 17.5 and 16S RNAs are detected. 16 and 17.5S RNAs may be derived from the cleavage of 19S during subsequent nuclear processing steps. All of these molecules correspond to the late messenger region (LB, map unit 0.735 to 0.16). They are transported into the cytoplasm within 80 min after their synthesis.

The heterogeneity of viral species seen in the cytoplasm and nucleus after various chase times was reproducibly observed. This is somewhat different from those reports obtained by others (3, 29). It is possible that our chase conditions minimize the accumulation of counts in major species that may occur during a long pulse. Such an accumulation of a major species could mask the detection of minor viral RNA species.

By comparing the profiles in the sucrose gradients of various cytoplasmic and nuclear viral species after different chase times, it is likely that cytoplasmic 19S is transported as such from the nucleus. 19S RNA is the predominant cytoplasmic species seen in the short chase, whereas 16S is the predominant species in the longer chase. These results are in good agreement with those by Aloni et al. (3). The precursor-product relationship between the cytoplasmic 19 and 16S is not obvious. 16S RNA is observed in the cytoplasm after a 10- to 15-min chase where there are only 19 and 17.5S RNAs in the nucleus (Fig. 4a and b, and 3c and d). We do detect

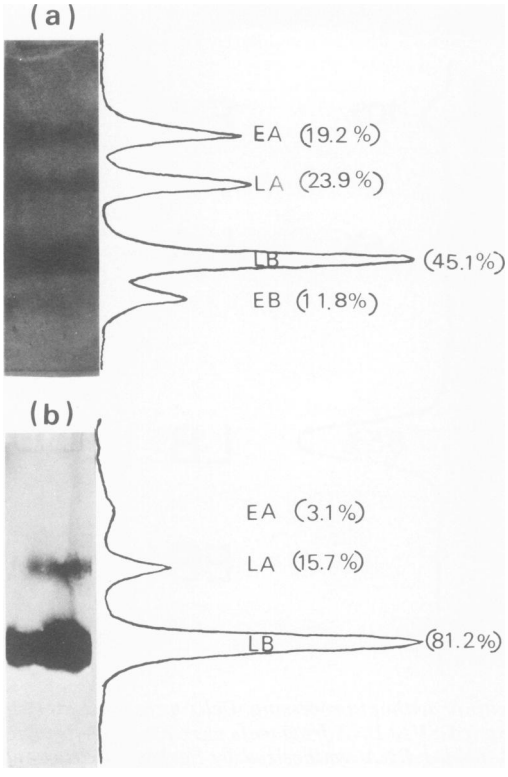

FIG. 6. *Sequence specificities of nuclear RNAs with half-lives of 40 min (16 to 19S) and 3 h (2 to 4S). Nuclear RNA was isolated from two petri dishes 45 h postinfection after a 5-min pulse with [^{3}H]uridine and a 1-h chase. The RNA sample was sedimented through a 5 to 20% sucrose gradient. Fractions of 16 to 19S and 2 to 4S RNAs were pooled separately and hybridized to strips of 1 μg of single-stranded SV40 DNA fragments. (a) RNA of sizes 2 to 4S; (b) RNA of sizes 16 to 19S.*

significant amounts of 16S in the nucleus at 30 min of chase and thereafter (Fig. 3e and f). If we compare the amounts of labeling of cytoplasmic viral RNA at the 0- and 5-min chase times with the labeling of nuclear viral RNA at these same times (Table 1), we can conclude that we have less than 1% cross-contamination. The distinct sedimentation profiles of nuclear and cytoplasmic viral RNA after a 6-h chase (Fig. 3h and 4f) also indicate that cross-contamination is not a problem. Therefore, viral nuclear 16S RNA cannot be the consequence of cytoplasmic contamination. We cannot exclude the possibility that nuclear 16S may be a nonspecific degradation product. However, the reproducible appearance of a unique 16S nuclear peak at various later chase time intervals (Fig. 3) strongly suggests that it is not so. 16S RNA may be cleaved from the larger viral species by a mechanism such as splicing (2, 4, 7) within the nucleus followed by its rapid transport into the cytoplasm. This would be analogous to ribosomal 28 and 18S, which are also rapidly transported and cannot be detected in the nucleus (20). Alternatively, cleavage of larger viral RNA species into 16S RNA may proceed in both nucleus and cytoplasm. The data that we have do not permit a definite conclusion.

The 2 to 4S labeled nuclear viral RNA, representing 10% of the initial nuclear viral RNA labeling, seems to be a mixed population derived from various nuclear processing steps. Forty percent of these molecules hybridize equally to both the early and late strands of the *Bam* I–*Hpa* II-A fragment with map unit 0.16 to 0.735 (EA and LA, see Fig. 6a). It is possible that they are RNAs coded for by pallindromic regions that correspond to nonmessenger regions of the late-strand primary transcript. Because the hairpins have approximate twofold axes of symmetry, these late nonmessenger fragments would hybridize efficiently with both early and late strands. These hairpins may include regions of map unit 0.68 ± 0.03, 0.17 ± 0.02, and 0.26 ± 0.02 in A, C, G, and B *Hin* II, -III digest fragments (13, 26, 28). Similar hairpin structures may also be found in the early-strand nonmessenger region. Hairpin regions would be more resistant to degradation, and, therefore, they would have a long half-life and generate a much larger intranuclear pool. A large unlabeled 2 to 4S pool may partly explain why labeled 2 to 4S RNAs appear only after a 30-min to 1-h chase. Approximately 40% of the small RNAs are specific to only the messenger region (LB, map unit 0.735 to 0.16) of the late strand. These RNA fragments may be the side products of subsequent nuclear processing steps such as cleavage of nuclear 19S to 17.5 and 16S. Because these cleavage steps are detected at 15 to 60 min after a chase, this may also explain why the small nuclear viral RNAs appear after a 30-min chase time interval.

The various steps of selecting transcribed sequences for messengers from the nucleus to the cytoplasm are important in the control of gene expression (16, 17). Further studies will be needed to determine, in detail, these processing mechanisms and possible biological functions of the RNA sequences restricted in the nucleus.

ACKNOWLEDGMENTS

We thank Marshall Bloom, Michael Seidman, and Cha-Mer Wei for their helpful suggestions.

LITERATURE CITED

1. **Acheson, N. H.** 1976. Transcription during productive infection with polyoma virus and simian virus 40. Cell 8:1–12.
2. **Aloni, Y., R. Dhar, O. Laub, M. Horowitz, and G. Khoury.** 1977. Novel mechanism for RNA maturation: the leader sequences of simian virus 40 mRNA are not

transcribed adjacent to the coding sequences. Proc. Natl. Acad. Sci. U.S.A. **74**:3686-3690.

3. **Aloni, Y., M. Shani, and Y. Reuveni.** 1975. RNAs of simian virus 40 in productively infected monkey cells: kinetics of formation and decay in enucleated cells. Proc. Natl. Acad. Sci. U. S. A. **72**:2587-2591.
4. **Berget, S. M., C. Moore, and A. P. Sharp.** 1977. Spliced segments at the 5'-terminus of adenovirus 2 late mRNA. Proc. Natl. Acad. Sci. U.S.A. **74**:3171-3175.
5. **Berk, A. J., and P. A. Sharp.** 1978. Spliced early mRNA of simian virus 40. Proc. Natl. Acad. Sci. U.S.A. **75**:1274-1278.
6. **Birkenmeir, E., E. May, and N. P. Salzman.** 1977. Characterization of simian virus 40 *tsA*58 transcriptional intermediates at restrictive temperatures: relationship between DNA replication and transcription. J. Virol. **22**:702-710.
7. **Chow, L. T., R. E. Gelinas, T. R. Broker, and R. T. Roberts.** 1977. An amazing sequence arrangement at the 5' ends of adenovirus 2 messenger RNA. Cell **12**:1-8.
8. **Condit, R. C., A. Cowie, and R. Kamen.** 1977. Polyoma virus transcription *in vitro*. J. Mol. Biol. **115**:215-235.
9. **Darnell, J. E., W. R. Jelinek, and G. R. Molloy.** 1973. Biogenesis of mRNA: genetic regulation in mammalian cells. Science **181**:1215-1221.
10. **Derman, E., and J. E. Darnell.** 1974. Relationship of chain transcription to poly(A) addition and processing of hnRNA in HeLa cells. Cell **3**:255-264.
11. **Gosh, P. K., V. B. Reddy, J. Swinscoe, P. V. Choudary, P. Lebowitz, and S. M. Weissman.** 1978. The 5'-terminal leader sequences of late 16S mRNA from cells infected with simian virus 40. J. Biol. Chem. **253**:3643-3647.
12. **Greenberg, H., and S. Penman.** 1966. Methylation and processing of ribosomal RNA in HeLa cells. J. Mol. Biol. **21**:527-535.
13. **Hsu, M.-T., and W. R. Jelinek.** 1977. Mapping of inverted repeated DNA sequences within the genome of simian virus 40. Proc. Natl. Acad. Sci. U.S.A. **74**:1631-1634.
14. **Laub, O., and Y. Aloni.** 1976. Transcription of simian virus 40. VI. SV40 DNA-RNA polymerase complex isolated from productively infected cells transcribed *in vitro*. Virology **75**:346-354.
15. **Levis, R., and S. Penman.** 1977. The metabolism of poly(A)$^+$ and poly(A)$^-$ hnRNA in cultured Drosophila cells studied with a rapid uridine pulse-chase. Cell **11**:105-113.
16. **Lewin, B.** 1975. Units of transcription and translation: the relationship between heterogeneous nuclear RNA and messenger RNA. Cell **4**:11-20.
17. **Lewin, B.** 1975. Units of transcription and translation: sequence components of heterogeneous nuclear RNA and messenger RNA. Cell **4**:77-94.
18. **May, E., H. Kopecka, and P. May.** 1975. Mapping the transcription site of the SV40-specific late 16S mRNA. Nucleic Acids Res. **2**:1995-2005.
19. **Meissner, H. C., J. Meyer, J. V. Maizel, Jr., and H. Westphal.** 1977. Visualization and mapping of late nuclear adenovirus RNA. Cell **10**:235-255.
20. **Penman, S.** 1966. RNA metabolism in the HeLa cell nucleus. J. Mol. Biol. **17**:117-130.
21. **Perry, R. P.** 1976. Processing of RNA. Annu. Rev. Biochem. **45**:605-629.
22. **Philippsen, P., and H. G. Zachau.** 1972. Partial degradation of transfer RNAs and transfer RNA fragments by spleen phosphodiesterase as studied by disc electrophoretic methods. Biochim. Biophys. Acta **277**: 523-538.
23. **Scherrer, K.** 1969. Isolation and sucrose gradient analysis of RNA, p. 413-432. *In* K. Habel and N. P. Salzman (ed.), Fundamental techniques in virology. Academic Press Inc., New York.
24. **Scholtissek, C.** 1971. Detection of an unstable RNA in chick fibroblasts after reduction of the UTP pool by glucosamine. Eur. J. Biochem. **24**:358-365.
25. **Shani, M., E. Birkenmeier, E. May, and N. P. Salzman.** 1977. Properties of simian virus 40 transcriptional intermediates isolated from nuclei of permissive cells. J. Virol. **23**:20-28.
26. **Shen, C. K., and J. E. Hearst.** 1977. Mapping of sequences with a 2-fold symmetry on the simian virus 40 genome: a photochemical crosslinking approach. Proc. Natl. Acad. Sci. U.S.A. **74**:1363-1367.
27. **Southern, E. M.** 1975. Detection of specific sequences among DNA fragments separated by gel electrophoresis. J. Mol. Biol. **98**:503-617.
28. **Subramanian, K. N., R. Dhar, and S. M. Weissman.** 1977. Nucleotide sequences of a fragment of SV40 DNA that contains the origin of DNA replication and specifies the 5' end of "early" and "late" viral RNA. J. Biol. Chem. **252**:355-367.
29. **Weinberg, R. A., S. O. Warnaar, and E. Winocour.** 1972. Isolation and characterization of simian virus 40 ribonucleic acid. J. Virol. **10**:193-201.
30. **Wertz, G. W.** 1975. Method of examining viral RNA metabolism in cells in culture: metabolism of vesicular stomatitis virus RNA. J. Virol. **16**:1340-1344.
31. **Zimmerman, S. B., and G. Sandeen.** 1966. The ribonuclease activity of crystallized pancreatic deoxyribonuclease. Anal. Biochem. **14**:269-277.